energies

MDPI

Article

Research on the Effect of an Air-Blown Interrupting Gap to Reduce the Rate of Lightning Tripping

Hao Li [1,*], Jufeng Wang [1], Ping Huang [1], Kezhu Guo [2] and Yanlei Wang [1]

[1] High Voltage Laboratory, Guangxi University, Nanning 530004, China
[2] State Grid Tacheng Power Supply Company, Tacheng 830000, China
* Correspondence: 2012392038@st.gxu.edu.cn

Abstract: The air-blown interrupting gap protection method is a self-energy interrupting method based on the concept of suppressing arc building by frequency continuation. In order to verify the effect of an air-blown interrupting gap to reduce the rate of line lightning tripping, in this paper, the protection principle of the air-blown interrupter gap is first described, and the action process simulated by COMSOL Multiphysics simulation software. Next, a frequency renewal test circuit is built for the test. Then, an arc-building rate calculation model and a lightning trip rate calculation model under the condition of an air-blown interrupting gap are established, and, finally, a 10 kV overhead line in Yunnan is selected for the verification of the calculation example. The results show the following: a gas blowing arc gap can be effectively extinguished in about 2.5 ms frequency arc and with no re-ignition phenomenon. Before and after the installation of the gas blowing arc gap line, the arc rate changed from 37.27% to 4.1%, respectively, and the lightning trip rate changed from 8.64 times/(40 thunderstorm days—100 km) to 0.337 times/(40 thunderstorm days—100 km), respectively. The decline rate was more than 95%, and in actual operation, it reduced the lightning trip rate enough to achieve good results.

Keywords: overhead transmission lines; air-blown arc extinguishing lightning protection gap; arc building rate; lightning strike trip rate

Citation: Li, H.; Wang, J.; Huang, P.; Guo, K.; Wang, Y. Research on the Effect of an Air-Blown Interrupting Gap to Reduce the Rate of Lightning Tripping. *Energies* **2023**, *16*, 1474. https://doi.org/10.3390/en16031474

Academic Editors: Richard Cselko and Bálint Németh

Received: 21 December 2022
Revised: 16 January 2023
Accepted: 26 January 2023
Published: 2 February 2023

1. Introduction

Overhead transmission lines, the largest element of the energy transmission equipment of the power grid, have been plagued by lightning strikes, affecting their safe operation. Overhead lines are susceptible to lightning trips due to complex erection terrain, wide distribution, and low insulation strength, causing line accidents and exposing their weak ability to resist lightning risks [1]. Lightning strikes are one of the most important factors in lightning tripping accidents on overhead lines [2]. According to statistics, Southern Power Grid Company 110 kV and above overhead line accident trips account for 66.81% of lightning trips; the National Grid Company 330 kV and above overhead line lightning trips account for up to 50.8% [3].

At present, there are two main methods of lightning strike protection: "Blocking type" and "Diversion type" [4]. "Blocking type" lightning protection is based on the concept that no flashover occurs during a lightning strike. "Diversion type" lightning protection is a concept that allows lightning flashes to occur and uses automatic reclosing devices to troubleshoot. "Blocking type" lightning protection limits the potential difference between the two ends of the insulator to achieve the purpose of no flashover by installing lightning rod, lightning wire and reducing the grounding resistance of the tower [5–7]. The lightning protection effect of installing lightning rods and lightning lines is affected by the terrain and climate. As the voltage level increases, its lightning protection effect will decrease, and may cause a line bypassing phenomenon [8,9]. The effectiveness of reducing the grounding resistance of a pole tower is influenced by the resistivity of the soil.

Reaching the standard with the final value of the reduced resistance is often not easy [10]. Methods of improving line insulation levels are influenced by economic factors, and specific processes are difficult to implement [11]. In the lightning protection process, metal oxide lightning arresters have hotspot challenges: substandard residual voltage and explosion-prone metal oxide valves. Such problems may affect the normal operation of the line [12,13]. "Diversion type" lightning protection is a protective gap installed in parallel at both ends of the insulator. This protective measure has the advantages of simple structure and high economy [14]. However, this method requires circuit breakers to achieve the purpose of cutting off the short-circuit current of industrial frequency. Parallel protection gaps may be burned out and cause protection failure. Traditional lightning protection measures essentially improve the level of lightning resistance, which does not effectively reduce the lightning trip rate, and there are hidden dangers in long-term operation. Therefore, it is paramount to reliably reduce the lightning trip rate and guarantee the safe and stable operation of power distribution lines.

The air-blown interrupting gap protection method is a new protection method developed by the authors' team. The concept of this method is to allow the formation process of flashover and broken-loop industrial frequency arcs to occur during lightning strikes. Before the automatic reclosing works, the arc has been extinguished to achieve the purpose of reducing the rate of lightning trips. This method uses air as the interrupting medium, so there is no risk of device explosion and non-standard residual pressure. Semi-enclosed structures' protection method of an air-blown arc extinguishing gap has been proposed in the literature [15]. Its arc path constraint, arc-arc column energy change, and the formation mechanism of expanding airflow have been described and the effectiveness of the gap for arc extinguishing by modeling simulation and test verified. One paper [16] showed the development and suppression mechanism of the I.F. current of the 110 kV line air-blown arc extinguishing device and found that the best period for arc extinguishment was within the first I.F. cycle. Another [17] analyzed the frequency renewal current blocking and lightning surge tests of compression interrupters, providing theoretical guidance for practical applications. Researchers [18] have considered the influence of the corner angle and compression tube size on the interrupting effect in the original structure and analyzed its competitive characteristics on the continuity of airflow energy and arc energy during the whole interrupting process through simulation optimization. Others [19] studied the energy conversion in the arc-extinguishing process of the long-gap gas lightning-protection device. Currently, this method has been qualified for actual operation in the national grid. The air-blown arc extinguishing devices have begun operating in other provinces in China, including Yunnan Province.

Based on the above, this paper focuses on the principle of air-blown interrupting gap and the effect of air-blown interrupting gaps in 10 kV overhead lines to reduce the lightning strike trip rate. First, the structure of the air-blown arc extinguishing device is introduced and the principle of air-blowing interrupting gap protection analyzed. Second, the action process is simulated using a simulation software and the whole dynamic change process analyzed. Then, a frequency continuity test is built and the interrupting effectiveness of the air-blown interrupting gap verified by the frequency continuity test. Finally, the calculation method of the lightning trip rate under the condition of air-blown arc extinguishing is built, and three 10 kV actual operating lines in Yunnan used as an example to compare the change of the lightning trip rate of the overhead line before and after the installation of an air-blown arc extinguishing gap.

2. Gas Blowing Interrupting Gap

The 10 kV air-blown interrupter gap was connected in parallel with the insulator being protected. The installation schematic is shown in Figure 1. The insulation fit made the air-blown interrupter gap discharge voltage lower than the breakdown voltage of the insulator string, and the gap was broken down to form a flashover channel in priority.

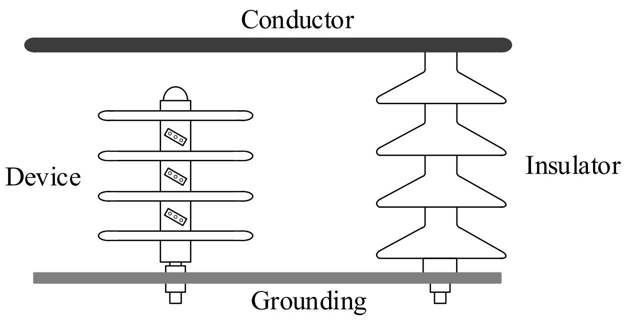

Figure 1. Schematic diagram of air-blown interrupter gap installation.

The interior of the device consisted of a number of compression tubes arranged in a spiral pattern, with adjacent compression tubes at 60° corners, as shown in Figure 2a. After a flashover occurs, the arc development path is confined within the compression tube. Air medium and arc coupling effect occurs. Under the action of mechanical compression, self-magnetic compression and fluid compression, pressure gradients, and temperature gradients are formed inside and outside the thin tube, generating a high-temperature, high-velocity airflow. The arc column inside the thin tube is driven by the gradient difference and injected outward, elongating the arc longitudinally, as shown in Figure 2b. At the same time, the spiral multi-tube structure will be a long arc divided into discontinuous multi-segment arcs. In the arc extinguishing nozzle, the arc column becomes expanded and dispersion, air medium radiation, convection, and other heat dissipation pathways reduce the arc column temperature. There is a sparse release of arc energy, inhibiting the process of flash build arc in the relay protection device before the action becomes frequency continuity arc blocking to ensure that lightning strikes do not trip.

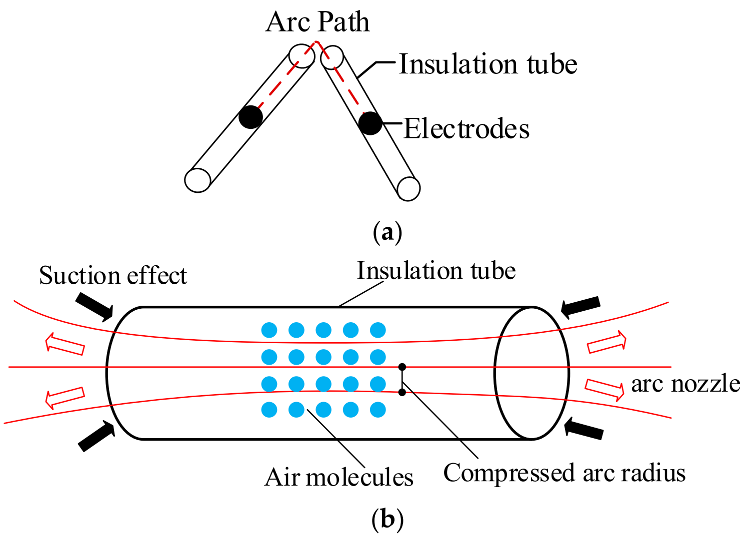

Figure 2. Schematic diagram of the internal space structure. (**a**) Insulation tube space structure; (**b**) effect on the arc.

3. Simulation Design

3.1. Geometric Models

The simulation in this paper chose the compression tube as the object of study and, as in each section of the arc extinguishing structure in the arc of the gas blowing process the compression tube was similar, COMSOL Multiphysics simulation software was used for two sections of the pipe for two-dimensional modeling, as shown in Figure 3. Figure 1 illustrates the insulating material, Figure 2 the air, Figure 3 the terminal, Figure 4 the ground terminal, and Figure 5 the metal electrode.

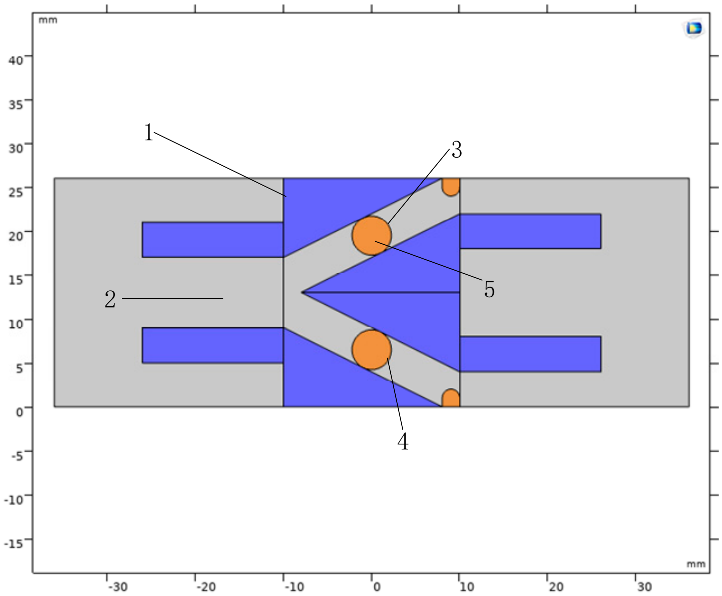

Figure 3. Two-dimensional model.

The initial temperature was set to 293.15 K; the pressure was 1 atm; a standard current waveform of 1.2/50 μs was applied to the terminal; the ground electrode potential was 0 V; there was no slip in the pipe wall; the current density was present in all materials except insulation; the simulation step was 0.01 ms; and the time was set to 10 ms.

3.2. Analysis of Simulation Results

The action process of the air-blowing interrupting gap was simulated, and the comparison and analysis considered the two aspects of temperature change and airflow speed change.

The temperature distribution of the air-blown arc extinguishing gap is shown in Figure 4. At 0.02 ms, the air gap was broken through and an arc channel was formed, at which time the arc temperature reached about 1600 K, as shown in Figure 4a. At 0.78 ms, as the arc current increased the radius of the arc column increased, the air inside the tube heated up sharply, and the highest temperature reached about 5000 K, as shown in Figure 4b. At 1.35 ms, the air inside the gap had formed a high-temperature energy body with a temperature of 10,000 K, and the arc energy was ejected to the external air with the airflow, as shown in Figure 4c. At 1.82 ms, we could clearly see the trend of the gas blowing arc. The arc and the air medium between the radiation, convection, and other heat exchange processes gradually caused the arc energy to decay, making the highest temperature inside the tube reach about 6000 K, as shown in Figure 4d. At 2.15 ms, the high-speed airflow took away most of the arc energy, and the temperature dropped to about 4300 K, as shown in Figure 4e. At 2.32 ms, the arc extinguishing process was basically over and the temperature at the airflow nozzle was about 2000 K. At this time, the arc was unable to maintain stable combustion and was gradually extinguished, as shown in Figure 4f. Continued observation showed the gas blowing arc gap did not undergo re-ignition.

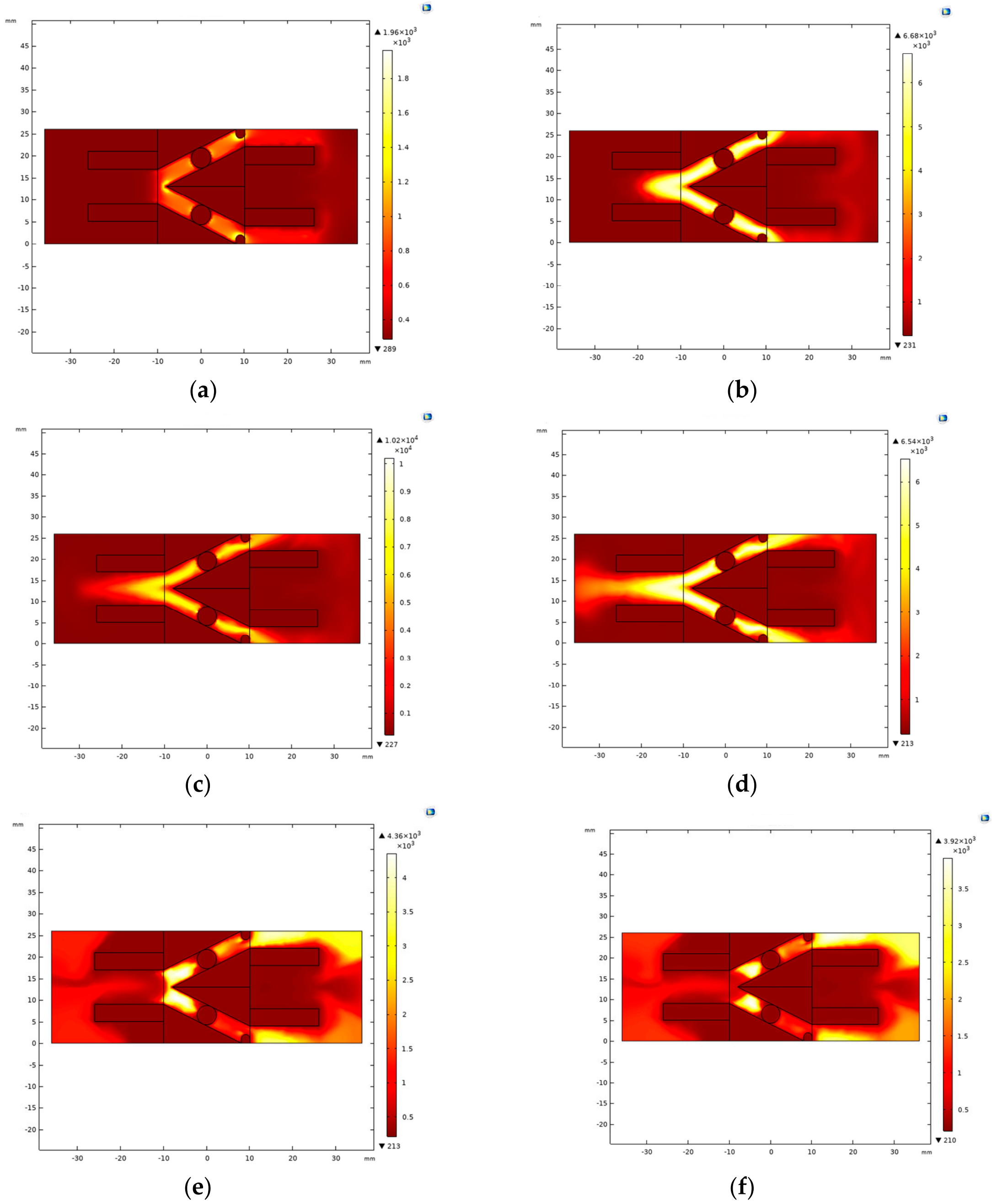

Figure 4. Map of the temperature distribution. (**a**) 0.02 ms, (**b**) 0.78 ms, (**c**) 1.35 ms, (**d**) 1.82 ms, (**e**) 2.15 ms, (**f**) 2.32 ms.

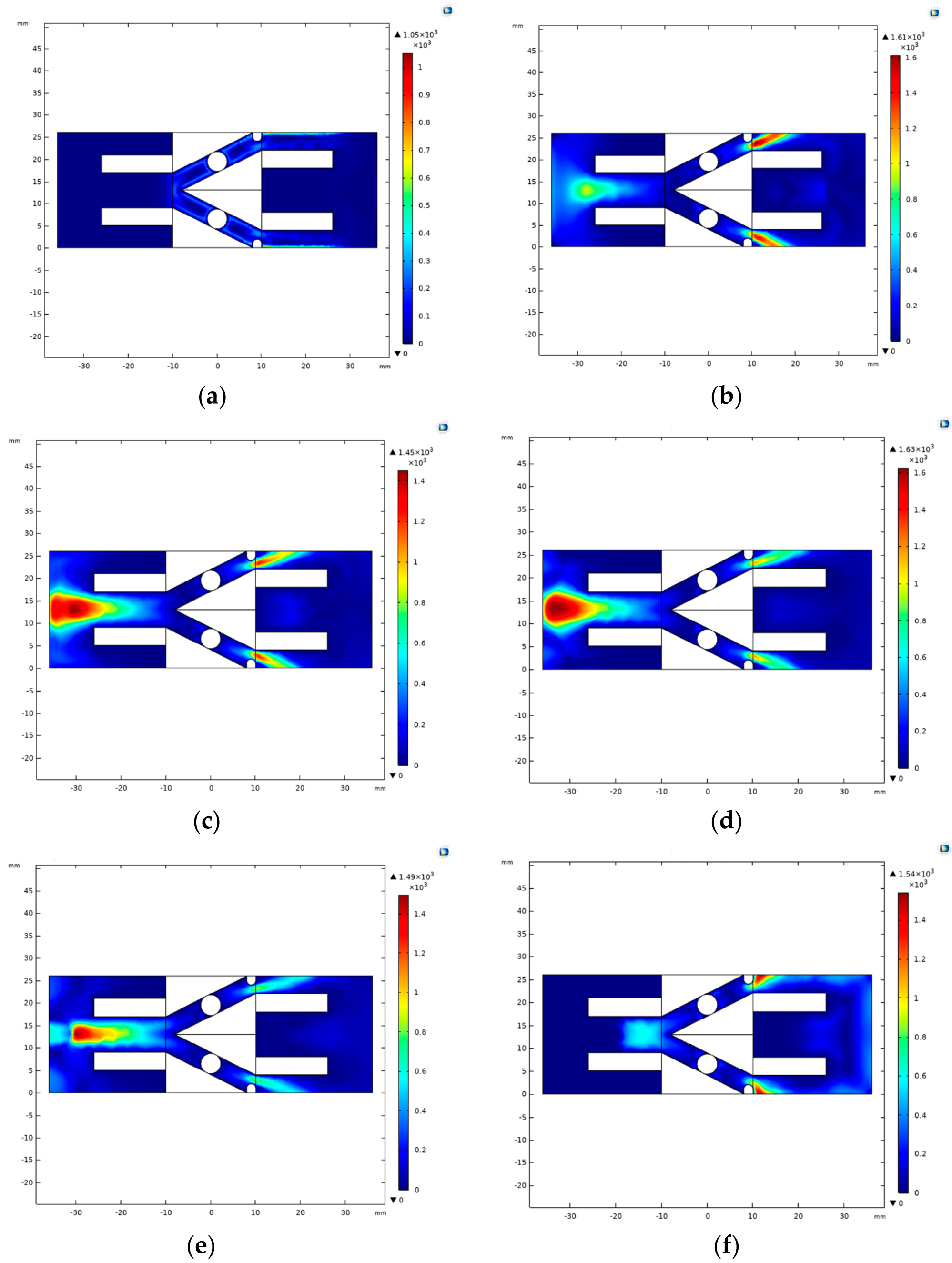

Figure 5. Map of the airflow velocity distribution. (**a**) 0.02 ms, (**b**) 0.78 ms, (**c**) 1.35 ms, (**d**) 1.82 ms, (**e**) 2.15 ms, (**f**) 2.32 ms.

Figure 5 shows the airflow change speed graph during the air blowing interrupting gap action. At 0.02 ms, the airflow in the pipe had begun to form a trend toward the nozzle, the speed was about 300 m/s, and with the increase in temperature, the airflow velocity also increased, reaching about 800 m/s at 0.78 ms, as shown in Figure 5a,b. At 1.35 ms, the high-speed airflow carrying arc energy was ejected at the nozzle, with a maximum airflow speed of about 1400 m/s, as shown in Figure 5c. At 1.82 ms, the change in airflow velocity lagged behind the change in temperature, and at this moment the airflow velocity reached a peak of about 1600 m/s and the air-blown arc trend was most obvious, as shown in Figure 5d. At 2.15 ms, with the consumption of arc energy, the trend of the air-blown arc had significantly weakened, and the airflow velocity had also gradually decreased to about 1000 m/s, as shown in Figure 5e. At 2.32 ms, the gas blowing arc extinguishing process had virtually ended, the airflow velocity at the structure nozzle was only 100 m/s, and the medium strength could be quickly restored, as shown in Figure 5f.

The key to extinguishing the arc with an air-blown arc gap is the arc energy and the energy of the arc extinguishing airflow. The energy of the arc extinguishing airflow adapts to the arc energy; the greater the energy carried by the arc itself, the greater the speed of the airflow generated. From Figures 4 and 5, the arc extinguishing airflow change lag with the change of temperature can be seen, which was due to the arc energy on the compressed duct energy air medium heating and other effects of the generation of the arc extinguishing airflow. In the entire arc extinguishing process, the strong arc extinguishing airflow continued to act on the arc under the constraints of the multi-inflection point structure, the long-distance large energy arc was divided into multiple easy-to-shade small arcs, the arc extinguishing airflow was always in the dominant position, the arc energy convection and de-freedom phenomenon was obvious, and the arc conductivity decreased. At the same time, the air-blown interrupter gap, interrupter medium for air, in the process of interrupting the arc, could quickly restore the dielectric insulation strength and in-depth inhibition of the continued development of the arc, until the arc was extinguished and inhibited arc reignition.

4. Air-Blowing Interrupting Gap Test

4.1. Industrial Frequency Renewal Current Test

To verify the interrupting capability of the air-blown interrupting gap, the latter was subjected to an industrial frequency continuity test. The test circuit diagram, built according to the requirements of the IEC 60099-8-2011 standard, is shown in Figure 6. The experimental circuit produced a standard lightning surge waveform of 1.2/50 μs and the IFT test circuit produced 10 full cycles of the rated voltage waveform with the frequency maintained at 50 Hz. The resulting IFT continuity was able to last for a period of time. The left side IG is the impact power circuit; C_1 is the main capacitor of the impact power circuit; S_1, S_2, and S_3 are the gaps; TO is the main body of the air-blown interrupter gap; CT is the current transformer; DMM is the measuring mechanism; T is the frequency power circuit; and T_1 is the frequency transformer.

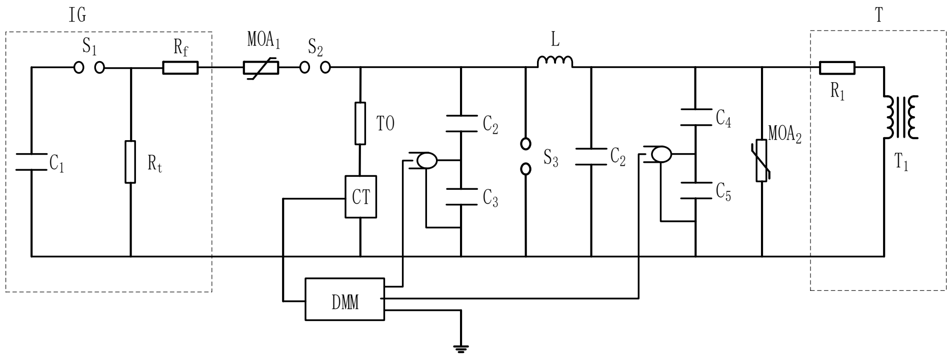

Figure 6. Power frequency freewheeling test circuit diagram.

Test Procedure

(1) The test circuit was built, as shown in Figure 6, the air-blown interrupter gap in parallel at both ends of the insulator was installed, as shown in Figure 1, and the air gap distance was adjusted to meet the insulation fit requirements.
(2) The frequency voltage at both ends of the test article and 13.2 kV frequency voltage at both ends of the 10 kV air-blown interrupter gap were pre-applied.
(3) After about 3 min, the left side of the shock power circuit was triggered to generate a lightning surge voltage, applied to both ends of the test product, and the voltage and current waveform and air blowing arc gap action process recorded. The frequency continuity test circuit was able to have a self-selected phase, and the test was selected in the frequency voltage waveform of the maximum positive half-cycle peak and the

maximum negative half-cycle peak moment trigger surge voltage waveform as an example. The waveform diagram is shown in Figure 7. CH1 is the voltage waveform, and CH2 is the current waveform.

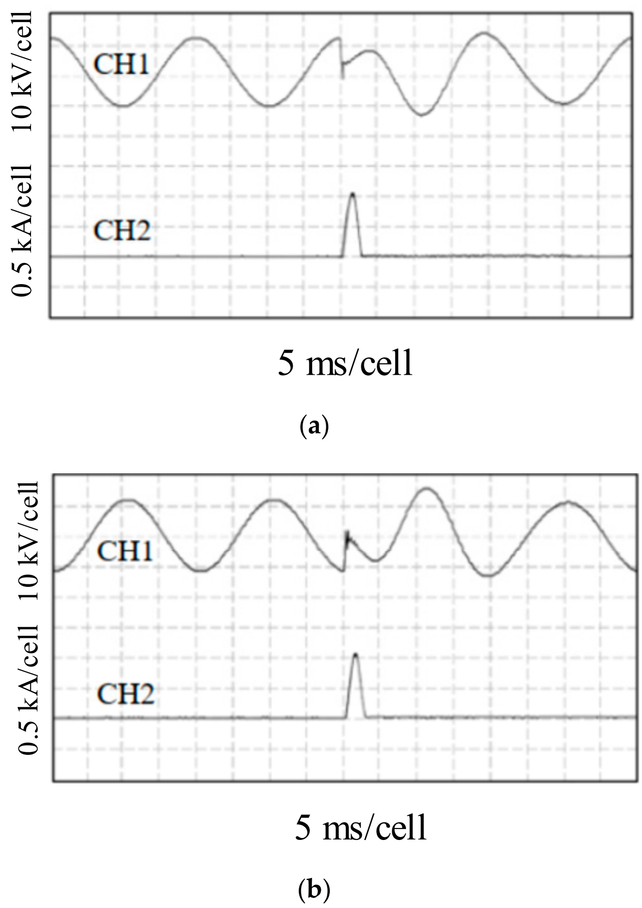

Figure 7. Test object voltage and current waveforms. (**a**) Positive polarity triggers the inrush voltage of the working frequency voltage; (**b**) negative polarity trigger shock voltage of the industrial frequency voltage.

As shown in Figure 7a, the lightning shock was applied at a frequency voltage of 90°. The gap formed a discharge breakdown channel and the voltage at both ends of the test piece decayed sharply from the peak value to a value near zero. When the air-blown arc gap extinguished the frequency arc, the voltage in 1.5 ms~2 ms or so returned to the first positive polarity of the peak, after a brief oscillation, to restore the normal amplitude and frequency. According to the current waveform, the peak value of the frequency continuation current of about 1.2 kA was reached at about 1.3 ms and dropped to zero at about 2.5 ms, indicating that the test product extinguished the frequency continuation current at about 2.5 ms, and no subsequent re-ignition occurred. From Figure 7b, the negative polarity trigger shock voltage changed in a similar fashion, the same current in about 2.5 ms extinguished the peak of about 1.2 kA of industrial frequency renewal current, and the subsequent voltage and frequency returned back to normal with no re-ignition phenomenon. During the experiment, the whole process of air-blowing gap action was recorded using a camera, as shown in Figure 8.

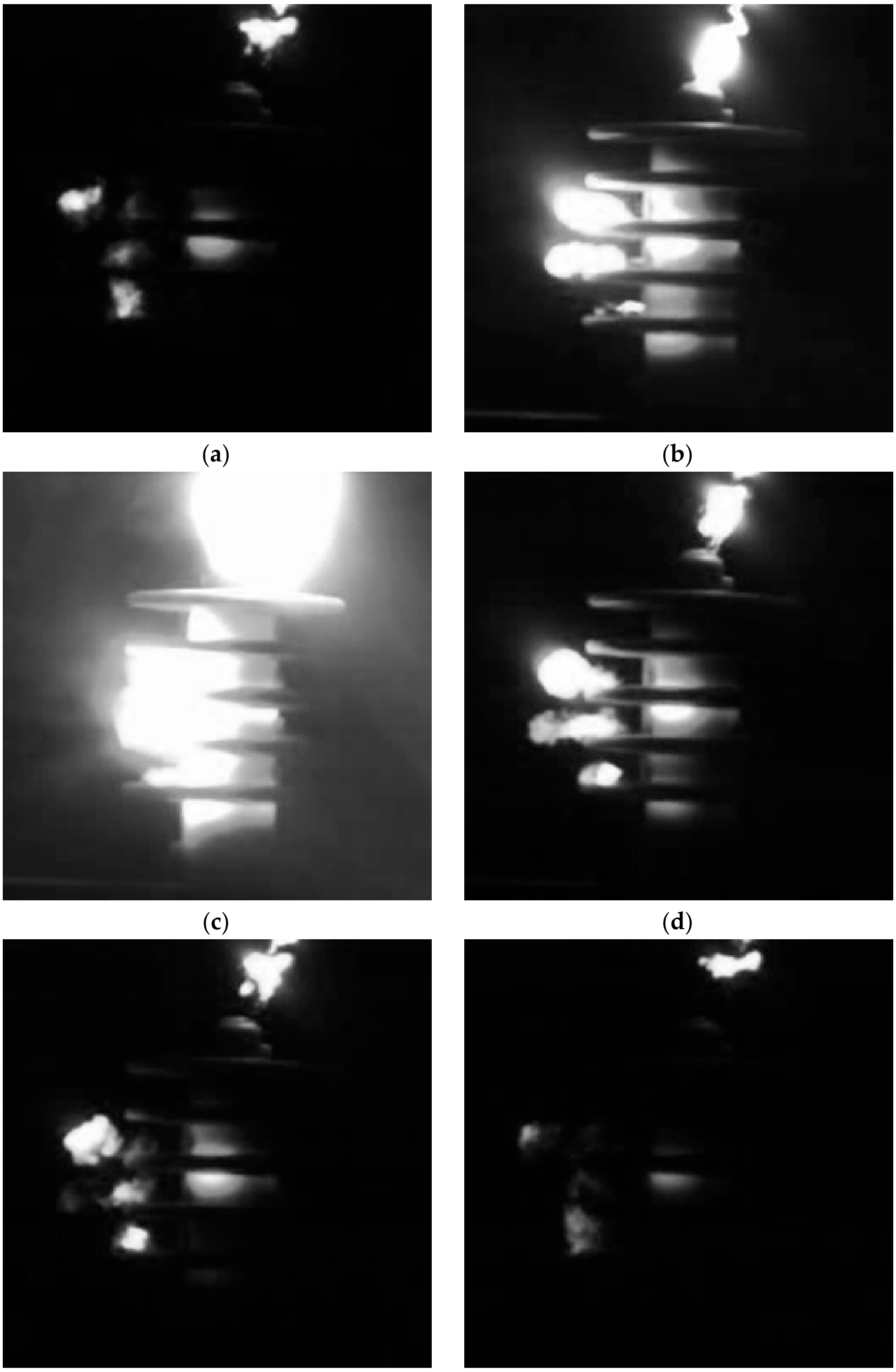

(**a**) (**b**) (**c**) (**d**) (**e**) (**f**)

Figure 8. Action diagram of the air blowing arc extinguishing gap. (**a**) The air gap was broken through and an arc channel was formed; (**b**) the air inside the tube heated up rapidly and the airflow started to form a trend towards the nozzle; (**c**) the air in the gap formed a high temperature energy body, at this time the most violent action; (**d**) the arc and the air medium between the radiation, convection, and other heat exchange processes gradually decayed the arc energy; (**e**) the trend of the air-blown arc was significantly weakened; (**f**) the arc was unable to maintain stable combustion, and was gradually extinguished.

The simulation results and the actual test results had some errors, but virtually matched. After analyzing the experimental data, the arc extinguishing time was selected as 3 ms in the following trip rate model, and the arc extinguishing process was considered to be completely finished after 3 ms.

5. Calculation of Lightning Strike Trip Rate

Lightning overhead line tripping is the root cause of damage to the relay device designed to respond to a lightning flash after the frequency arcing, causing the circuit breaker to trip. As the air-blown interrupter gap is intended to "allow the flash, not to allow the arc" as its concept, the depth of the arc-building process to suppress the frequency continuity, to achieve the goal of significantly reducing the lightning trip rate, is significant to the arc-building rate and lightning trip rate for modeling analysis and calculation.

5.1. Arc Building Rate

First, 30 repetitive tests were conducted for two amplitudes, 0.5 KA and 1.0 kA, respectively, and the test data were obtained as shown in Table 1. From the data of interrupting parameters in the table, it can be seen that the interrupting success rate of both amplitudes of the frequency current was maintained above 75%. The single interrupting success rate in the model in this paper was taken as 75%, which is considered to have achieved the ideal single interrupting success rate for this condition.

Table 1. Gas blowing arc extinguishing gap arc extinguishing parameters.

Industrial Frequency Current /kA	Arc Extinguishing Time /ms	Arc Extinguishing Success Rate/%
0.5	2.34	76.7
1.0	2.37	80.8

Considering that 10 kV overhead lines mostly use reinforced concrete towers and are neutral point ungrounded systems, the average operating voltage gradient is

$$E = \frac{U_{\mathrm{e}}}{2l_s} \tag{1}$$

In the Equation (1), U_{e} is the rated voltage and l_s is the insulator string length.

According to GB14285-2006, the fastest action time of a relay protection device in China is 10~20 ms. Therefore, when the single interrupting time of the air-blown interrupting gap is an approximate ideal of 3 ms, the probability of the action until the nth completed interrupting is

$$P_n = a(1-a)^{n-1}, n \le 3 \tag{2}$$

In the Equation (2), a is the single-action interrupting success rate.

Since in the air-blown interrupting gap each interrupting action is independent of the others, the effective arc-building factor K is

$$K = 1 - \sum_{n=1}^{3} P_n = 1 - a^3 + 3a^2 - 3a \tag{3}$$

For the overhead line without the installation of a gas blowing arc extinguishing device, the impact flashover after the formation of the frequency arc in natural conditions with uncertainty of extinguishing time was considered. In the line where the air-blown interrupter gap was installed, the arc is intervened by strong airflow in the arc-building process at the impact arc stage, and the arc-building rate is

$$\eta = K \times \left(4.5\mathrm{E}^{0.75} - 14\right) \times (1-\zeta) \tag{4}$$

In the Equation (4), ζ is the arc building inhibition rate, and the variation law of the arc building rate and effective arc building factor are shown in Figure 9. It can be seen that the larger the value of the effective arc building factor K, the larger the growth rate of the variation of the arc building rate and the more detrimental to the suppression of the arc building process. Under this test condition, the effective arc building factor corresponding to the single arc extinguishing success rate of 75% was about 0.01, and the amplitude and growth rate of the arc building rate were very small, which ensured the most ideal arc extinguishing effect to the maximum extent.

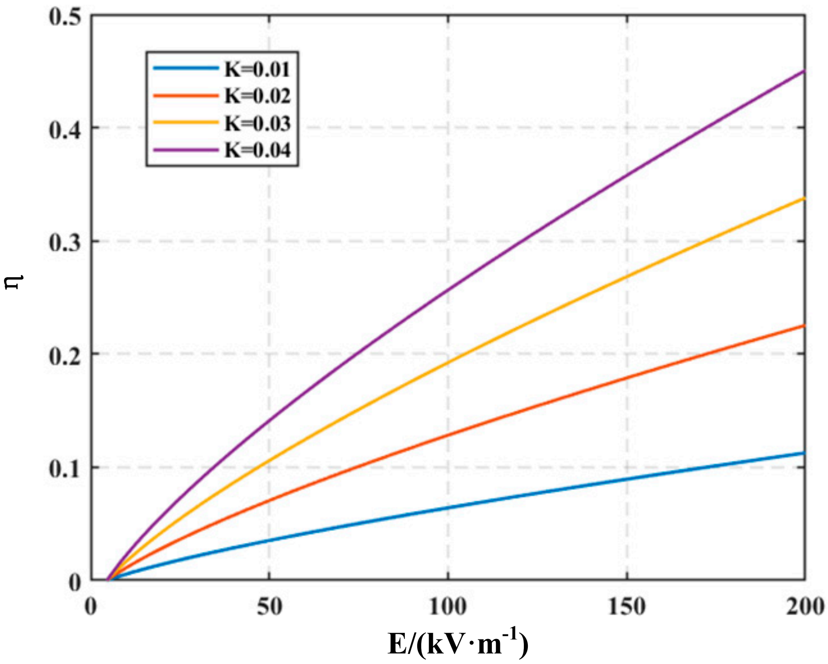

Figure 9. Variation trend of the arc establishment rate and arc establishment coefficient.

5.2. Lightning Strike Trip Rate

Lightning strike trip rate ground analysis methods include the gauge method, electrical geometry method, and pilot development model method. The basic parameters of the electrical geometry method are the lightning pilot strike distance, line and tower height, etc., which are mainly applied in the calculation of the shielding range of the lightning protection line and the line bypass rate. The pilot development model is mainly applied to the lightning upstream and downstream pilot development process to optimize the parameters for the calculation of the line bypass rate. The protection effect of the air-blown interrupter gap is independent of line length, lightning line shielding effect, ground network grounding resistance, and other factors, so the regulation method is used for modeling calculations. The premise is that the overhead line towers are installed with an air-blown interrupter gap.

The number of air-blown arc extinguishing lightning trips on 10 kV overhead lines was calculated [20,21] and can be expressed through the following:

According to the regulations, for areas with occurrences of thunderstorm greater than 20 days, the lightning current magnitude probability can be calculated by the empirical Equation (5):

$$\lg P = -\frac{I}{88} \tag{5}$$

In Equation (5), P is the probability that the lightning current amplitude exceeds I.

The number of lightning strikes encountered on overhead lines N is

$$N = \gamma \times \frac{A}{1000} \times L \times T_{\mathrm{d}} \tag{6}$$

In Equation (6), γ is the average annual falling lightning density; A is the equivalent of the width subject to lightning, and its value is approximately proportional to the height of the conductor $\mathrm{h_d}$, $A \approx 10\mathrm{h_d}$; L is the line length; and T_d is the average annual number of thunderstorm days.

Without considering the shunt coefficient and coupling coefficient, the lightning resistance level I_1 of the distribution line lightning rod tower and the lightning resistance level I_2 of the lightning conductor are

$$I_1 = \frac{U_{50\%}}{R_{\mathrm{ch}} + \frac{L_{\mathrm{gt}}}{2.6} + \frac{\mathrm{h_d}}{2.6}} \tag{7}$$

$$I_2 = \frac{U_{50\%}}{100} \tag{8}$$

In Equations (7) and (8), $U_{50\%}$ is the lightning impact discharge voltage; R_{ch} is the impact grounding resistance; and $\mathrm{h_d}$ is the height of the wire.

The numbers of line trips caused by lightning strikes on towers and conductors are

$$n_1 = N\mathrm{g}P_1\eta \tag{9}$$

$$n_2 = N(1-\mathrm{g})P_2\eta \tag{10}$$

In Equations (9) and (10), n_1 is the number of lightning tower trips; n_2 is the number of lightning trips on the wire; g is the rate of hitting the pole, including its value and the topography of overhead lines.

6. Example Analysis

An example is given of a 10 kV overhead line in Yunnan, China, located in a mountainous area with high soil resistivity. The entire line is not equipped with lightning protection lines and is prone to lightning strikes. In 2021, the line was retrofitted with lightning protection and an air-blown interrupting lightning protection gap was installed. The line reference parameters are shown in Table 2.

Table 2. The 10 kV overhead distribution line parameters.

Title	Reference Values	Unit
Line length	100	km
Annual thunderstorm days	40	d
Falling lightning density	0.018	times/km^2·T$_\mathrm{d}$
Tower inductors	4.95	μH
Grounding resistance	25	Ω
Stroke rate	0.5	g
Insulator length	0.195	m

For this 10 kV overhead line, the pin insulator height l_s was 0.195 m and the average operating voltage gradient is

$$E = \frac{10}{2 \times 0.195} = 25.64\ \mathrm{kV/m} \tag{11}$$

The arc-building rate η_1 before and after the installation of the air-blown arc extinguishing device is

$$\eta_1 = \left(4.5 \times 25.64^{0.75} - 14\right) \times 10^{-2} = 0.3727 \tag{12}$$

The arc building rate η_2 before and after installation of the air-blown arc extinguishing device is

$$\eta_2 = 0.01 \times \left(4.5 \times 25.64^{0.75} - 14\right) \times (1 - 0.89) = 0.041 \tag{13}$$

Obviously, in overhead lines with a gas blowing arc gap, the arc-building rate achieved a substantial reduction from the original 37.27% down to only about 4.1% of the original level. This showed that it was difficult to realize the arc building process under the action of the air blowing interrupting gap, which can effectively improve the arc building rate of the line.

On 40 thunderstorm days per year, the number of lightning strikes encountered on the overhead lines of a 100 km line is

$$N = 0.018 \times \frac{10 \times 12}{1000} \times 100 \times 40 = 8.64 \tag{14}$$

Lightning strike tower lightning resistance level I_1 and lightning strike conductor lightning resistance level I_2 can be calculated as follows:

$$I_1 = \frac{92.045}{25 + \frac{4.95}{2.6} + \frac{10}{2.6}} = 2.993 \text{ kA} \tag{15}$$

$$I_2 = \frac{92.045}{100} = 0.920 \text{ kA} \tag{16}$$

The probability that the lightning current amplitude exceeds I_1 and I_2 is

$$P_1 = 10^{-2.993/88} = 0.925 \tag{17}$$

$$P_2 = 10^{-0.920/88} = 0.976 \tag{18}$$

The numbers of line trips caused by lightning strikes on towers and conductors are

$$n_1 = 8.64 \times \frac{1}{2} \times 0.925 \times 0.041 = 0.164 \tag{19}$$

$$n_2 = 8.64 \times \left(1 - \frac{1}{2}\right) \times 0.976 \times 0.041 = 0.173 \tag{20}$$

The total number of trips on this 10 kV overhead line without lightning protection line is

$$n = n_1 + n_2 = 0.164 + 0.173 = 0.337 \tag{21}$$

The original overhead line lightning tripped up to 8.64 times. After the use of the gas blowing arc gap, lightning trips were down more than 95%. According to the actual operation of the line lightning monitoring data for more than a year, in the air-blowing arc protection gap protection, no lightning tripping accidents occurred in the actual operation of the line, indicating a significantly reduced rate of lightning tripping. This verified the effectiveness of the air-blown arc extinguishing device to effectively reduce the rate of lightning trips.

Actual Working Situation

In March 2021, the power grid company in Yunnan province installed 501 (167 towers) air-blown interrupting protection gap devices on 10 kv overhead lines. These devices are installed on the "panjiang" Line (P-J Line), the "laohuang" Line (L-H Line), and the "kelian" Line (K-L Line). Taking the K-L line as an example, the hanging network operation of the air-blown interrupting gap is shown in Figure 10.

(a) (b)

Figure 10. The hanging network operation of the air-blown interrupting gap. (**a**) Single-phase; (**b**) Three phase.

The three lines had a high number of lightning trips over the course of a year when the air-blown interrupting gap devices were not installed. Under the protection of the air-blown interrupting gap, the number of lightning trips is significantly reduced. The statistics on the number of lightning trips before and after the installation of air-blown interrupting gaps for the three lines is shown in Table 3. After the use of the gas blowing arc gap, the average drop in lightning trips is more than 90%. According to the operational effectiveness report provided by the company, the air-blown interrupting gap does not appear to be damaged and has achieved good operating results.

Table 3. Statistics on the number of lightning trips before and after installation.

Line	Statistics Time	The Number of Lightning Trips		
		A	B	C
P-J Line	2020.3–2021.3	4	2	3
	2021.3–2022.3	0	1	0
L-H Line	2020.3–2021.3	2	4	1
	2021.3–2022.3	0	0	0
K-L Line	2020.3–2021.3	2	3	5
	2021.3–2022.3	1	1	0

7. Conclusions

(1) The air-blown interrupting gap protection method is a new protection method developed by the authors' team. The method relies on the arc building process of suppressing the frequency continuation current before the relay protection device operates to reduce the lightning strike trip rate.

(2) Through the simulation software to simulate the arc extinguishing process and the industrial frequency continuity test, an air-blown interrupter gap at 2.5~3 ms reliably extinguished the frequency arc and did not show reignition. Compared with the action time of relay device, the method presented herein has faster action time.

(3) A lightning strike trip rate calculation method is provided under the condition of air-blown arc extinguishing gap with the arc building rate as an important indicator. The installation of the gas blowing arc gap altered the arc-building rate from 37.27% down to about 4.1%, and the lightning trip rate from 8.64 times/(40 thunderstorm days—100 km) down to 0.337 times/(40 thunderstorm days—100 km), a decline of more than 95%. During the year of actual grid operation, the average drop in lightning trips is more than 90%. The effect of reducing the lightning trip rate was significant, and good results were achieved in reducing the lightning trip rate in actual operation.

Author Contributions: Conceptualization, J.W.; methodology, H.L. and J.W.; software, H.L.; validation, H.L., Y.W. and P.H.; formal analysis, H.L.; investigation, K.G.; resources, H.L., Y.W. and P.H.; data curation, H.L.; writing—original draft preparation, H.L.; writing—review and editing, H.L., Y.W. and P.H.; visualization, H.L.; supervision, Y.W. and P.H.; project administration, J.W.; funding acquisition, J.W., Y.W. and P.H. All authors have read and agreed to the published version of the manuscript.

Funding: This research was funded by the Guangxi Innovation-driven Development Project (major science and technology projects) number AA18242050.

Institutional Review Board Statement: Not applicable.

Informed Consent Statement: Not applicable.

Data Availability Statement: Not applicable.

Conflicts of Interest: The authors declare no conflict of interest.

References

1. Yi, H.; Cui, J. The present state and lightning protection of transmission line in China. *High Volt. Technol.* **2001**, *6*, 44–45+50.
2. Zhen, L. Analysis of the causes of tripping of 10kV lines in agricultural networks. *China High-Tech* **2022**, *3*, 29–30.
3. Chen, J.; Zhao, C.; Gu, S.; Xiang, N.; Wang, Y.; Lei, M. Status quo and development trend of lightning monitoring and protection technology in my country's power grid. *High Volt. Technol.* **2016**, *42*, 3361–3375.
4. Chen, W.; Sun, Z.; Wang, X.; Li, Q.; Yan, X.; Wang, F.; Li, H.; Wang, S.; Wang, Z.; Zhang, W. Study on Shunt Gap Lightning Protection for 35kV Overhead Transmission Lines. *Power Syst. Technol.* **2007**, *31*, 61–65.
5. Wang, C.; Zhu, L.; Ji, S.; Zhang, Q. Status and development of lightning protection for high-voltage transmission lines and substations. *Electr. Porcelain Light. Arrester* **2010**, *3*, 35–46.
6. Zhang, J.; Jin, M.; Cheng, Y.; Wang, H.; Xu, Y.; Zhang, Z.; Zhang, C.; Gan, P.; Yan, X. Selection of protection angle of lightning arrester for 10 kV insulated overhead lines. *Electr. Porcelain Light. Arrester* **2019**, *2*, 84–89. [CrossRef]
7. Peng, X.; Li, Z.; Li, Z.; Wang, X.; Yu, Z.; He, J. Effect of tower grounding resistance on the lightning protection performance of multiple lines with the same tower. *High Volt. Technol.* **2011**, *37*, 3113–3119.
8. Du, L.; Chen, H.; Chen, S.; Luo, T.; Li, J. Identification Method of shielding Failure and Back Striking for Overhead Transmission Line. *High Volt. Eng.* **2014**, *40*, 2885–2893.
9. Chen, Y.; Lin, K.; Li, Y. Study on protection Effectiveness of Early Streamer Emission Lightning Protection Systems. In Proceedings of the 2017 International Conference on Manufacturing Engineering and Intelligent Materials (ICMEIM 2017), Guangzhou, China, 25–26 February 2017.
10. Zhang, B.; He, J.; Zeng, R. State of art and prospect of grounding technology in power system. *High Volt. Eng.* **2015**, *41*, 2569–2582.
11. Li, Z.; Chen, W.; Zhang, T.; Dai, M.; Jiang, W.; Wang, C.; Liu, Z. Electrical structure design of lattice composite material tower of 110kV double circuit transmission line. *Power Syst. Technol.* **2015**, *39*, 536–542.
12. He, J.; Liu, J.; Hu, J.; Long, W.-C. Development of ZnO varistors in metal oxide arrestors utilized in Ultra High Voltage System. *High Voltage Eng.* **2011**, *37*, 634–643.
13. Zhou, W.; Zhang, S.; Zhang, L.; Feng, K.; Lin, J.; Wu, K.; Liu, W.; Li, J.; Li, S. Investigation on the Statistical deviation of residual voltage for ZnO—Based varistors under Impulse currents. *Insul. Surge Arresters* **2020**, *1*, 16–22.
14. Ge, D.; Feng, H.; Yuan, L.; Liu, J.; Zhang, C.-X.; Li, H. Experimental research on large power frequency current of parallel gap of insulator strings. *High Volt. Eng.* **2008**, *7*, 1499–1503.
15. Chen, Y.; Wang, J.; Huang, P.; Wang, Y.; Zhang, Y. Arc-extinguishing characteristics of semi-enclosed structures based on theory of positive shock wave reflection. *AIP Adv.* **2022**, *12*, 015009. [CrossRef]
16. Wang, J.; Han, L.; Lu, X.; Li, Z.; Zhang, Q. Research on the development and suppression mechanism of power frequency arc based on the gas blowing arc extinguishing model. *Electr. Meas. Instrum.* **2021**, *58*, 104–109.
17. Mao, C.; Wang, J.; Zhou, Y.; Meng, W.; Han, L. Experimental Research on Power Frequency Freewheeling Interruption and Lightning Impulse of Compression Arc Extinguishing Lightning Protection Device for 10kV Distribution Network. *Electr. Meas. Instrum.* **2022**, *59*, 38–44.
18. Wang, J.; Zhou, X.; Wang, Z.; Li, Z.; Han, L. Simulation optimization of arc suppression by self-energy multi-fracture structure. *Power Grid Technol.* **2019**, *43*, 739–745.
19. He, Q.; Wang, J.; Lu, Y.; Song, Y.; Jia, Z.; Li, H.; Wang, Y.; Zhang, Y. Research on Energy Conversion in the Arc-Extinguishing Process of a Long-Gap Gas Lightning-Protection Device. *Energies* **2022**, *15*, 7490. [CrossRef]

20. Yan, W.; Xiao, C.; Wu, X.; Li, J.; Tang, X.; Yang, F. Calculation of Lightning Trip Rate of 10 kV Distribution Line Based on Lightning Activity Characteristics. *High Volt. Technol.* **2021**, *47*, 1118–1127.
21. Liu, H.; Han, Y.; Chen, C.; Chen, Y.; Cheng, Z.; Li, L. Calculation of Lightning Trip Rate of Distribution Lines and Research on Differentiated Lightning Protection Methods. *Electr. Ceram. Surge Arrester* **2020**, *4*, 7–13+26.